Organic Electronics 13 (2012) 483–490

Contents lists available at SciVerse ScienceDirect

Organic Electronics

journal homepage: www.elsevier.com/locate/orgel

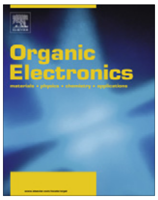

Efficient and color-stable solid-state white light-emitting electrochemical cells employing red color conversion layers

Hung-Bao Wu [a], Hsiao-Fan Chen [b], Chih-Teng Liao [a], Hai-Ching Su [a,*], Ken-Tsung Wong [b,*]

[a] Institute of Lighting and Energy Photonics, National Chiao Tung University, Tainan 71150, Taiwan
[b] Department of Chemistry, National Taiwan University, Taipei 10617, Taiwan

ARTICLE INFO

Article history:
Received 25 October 2011
Received in revised form 8 December 2011
Accepted 11 December 2011
Available online 3 January 2012

Keywords:
Light-emitting electrochemical cells
Color conversion layer
White light

ABSTRACT

We report efficient and color-stable white light-emitting electrochemical cells (LECs) by combining single-layered blue-emitting LECs with red-emitting color conversion layers (CCLs) on the inverse side of the glass substrate. By judicious choosing of the red-emitting dye doped in CCLs, good spectral overlap between the absorption spectrum of the red-emitting dye and the emission spectrum of the blue-emitting emissive material results in efficient energy transfer and thus sufficient down-converted red emission at low doping concentrations of the red-emitting dye in the CCLs. Low doping concentration is beneficial in reducing self-quenching of the red-emitting dye, rendering efficient red emission. Electroluminescent (EL) measurements show that the peak external quantum efficiency and the peak power efficiency of the white LECs employing red CCLs reach 5.93% and 15.34 lm W^{-1}, respectively, which are among the highest reported for white LECs. Furthermore, these devices exhibit bias-insensitive white EL spectra, which are required for practical applications, due to nondoped emissive layers. These results reveal that single-layered blue-emitting LECs combined with red-emitting CCLs are one of the potential candidates for efficient and color-stable white light-emitting devices.

© 2011 Elsevier B.V. All rights reserved.

1. Introduction

White organic light-emitting diodes (OLEDs) based on polymers and small-molecule materials have attracted intense attention due to their potential applications in flat-panel displays and solid-state lighting [1–5]. Recently, a power efficiency of white OLEDs higher than 120 lm W^{-1} has been reported by Reineke et al. under laboratory conditions [6]. However, multi-layered structure and chemically *p*- and *n*-doped transporting layers for reducing operating voltages complicate fabrication processes. Compared with conventional white OLEDs, solid-state white light-emitting electrochemical cells (LECs) possess several promising advantages. In solid-state LECs [7,8], electrochemically doped regions, i.e. *p*-type doping near the anode and *n*-type doping near the cathode, induced by spatially separated ions under a bias form Ohmic contacts with electrodes, giving balanced carrier injection, low operating voltages, and consequently high power efficiencies [7,8]. Therefore, LECs generally require only a single emissive layer, which can be easily deposited by solution processes and can conveniently utilize air-stable electrodes, e.g., Au and Ag, while OLEDs typically require more sophisticated multilayer structures and low-work-function cathodes for balanced carrier injection [1–5].

Solid-state white LECs based on a phase-separated polyfluorene/poly(ethylene oxide) (PEO) mixture exhibiting an external quantum efficiency (EQE) of 2.4% photons/electron were reported by Yang and Pei in 1997 [9]. Recently, white LECs based on excimer emission of a fluorene-oxadiazole copolymer with a current efficiency of 0.15 cd/A have been reported by Sun et al. [10]. However,

---

[*] Corresponding authors. Tel.: +886 6 3032121x57792; fax: +886 6 3032535 (H.-C. Su), tel.: +886 2 33661665; fax: +886 2 33661667 (K.-T. Wong).

E-mail addresses: haichingsu@mail.nctu.edu.tw (H.-C. Su), kenwong@ntu.edu.tw (K.-T. Wong).

1566-1199/$ - see front matter © 2011 Elsevier B.V. All rights reserved.
doi:10.1016/j.orgel.2011.12.011

moderate efficiencies of polymer LECs showed that the fluorescent nature of conjugated polymers limits the eventual electroluminescence (EL) efficiency due to the spin statistics. Compared with conventional polymer LECs that are usually composed of an emissive conjugated polymer, a salt and an ion-conducting polymer [7,8], LECs based on cationic transition metal complexes (CTMCs) show several further advantages and have attracted much attention in recent years [11–57]. In such devices, no ion-conducting material is needed since these CTMCs are intrinsically ionic. Furthermore, higher EL efficiencies are expected due to the phosphorescent nature of CTMCs. By employing a blue-emitting CTMC as the host and a red-emitting CTMC as the guest, solid-state white LECs with an EQE (power efficiency) of 4% (7.8 lm/W) were successfully demonstrated by Su et al. in 2008 [36]. Recently, improving the EQE (power efficiency) of CTMC-based white LECs up to 5.6% (11.2 lm/W) has been achieved by He et al. [42,47]. However, low photoluminescence quantum yields (PLQYs) (<0.2 even in dilute solutions) of the red-emitting CTMCs used in previously reported host–guest white LECs [36,42,47,55] preclude further enhancement in device efficiencies. Furthermore, single-layered host–guest white LECs usually suffer bias-dependent color shift, which is undesired for practical applications [36,42,55]. This phenomenon results from excitons formed by direct carrier trapping on the guest under relatively lower biases due to significant energy offsets in the energy levels between the host and the guest. Direct exciton formation on the red-emitting guest owing to charge trapping dominates EL emission under lower biases while exciton formation on the blue-emitting host followed by host–guest energy transfer tends to be more significant under higher biases. As a result, the EL emission of the single-layered host–guest white LECs changes from red to white as the bias slightly increases (2.9–3.3 V) [36,55] and such color instability prohibits their usage in practical applications.

Color stability under varying bias conditions is also a critical issue in white OLEDs and one of the reported practical ways to improve color stability is combination of blue-emitting devices with red color conversion layers (CCLs) on the reverse side of the glass substrates [58–61]. White emission can be generated by the superposition of nonabsorbed blue emission from the emissive layer and red emission, which is excited by the blue emission, from the CCLs. This approach can be implemented by easy fabrication techniques and can provide better color stability since only one emitter is present in the emissive layer, eliminating carrier trapping effect induced by the low-gap red-emitting dyes in host–guest white LECs [36,42]. Furthermore, highly efficient neutral red-emitting dye [4-(dicyanomethylene)-2-*t-butyl*-6-(1,1,7,7-tetramethyljulolidyl-9-enyl)-4H-pyran, DCJTB] suitable for use in OLEDs exhibits significantly deteriorated PLQYs (<0.1) in ionic emissive materials used as emissive layers of LECs due to environmental polarity while they show high PLQYs (>0.5) in neutral polymer films [51]. Since the PLQYs of the reported red-emitting CTMCs used in white LECs [36,42,47,55] are rather low (<0.2), utilizing neutral polymer CCLs doped with a highly efficient neutral red-emitting dye (DCJTB) would be beneficial in enhancing device efficiencies of white LECs. To the best of our knowledge, no white LEC composed of a blue-emitting device combined with a down-conversion red CCL has been reported. In this work, we demonstrate efficient and color-stable white LECs by combining single-layered blue-emitting LECs with red-emitting CCLs on the inverse side of the glass substrate. Photoluminescent (PL) measurements reveal that good spectral overlap between the absorption spectrum of the red-emitting dye and the emission spectrum of the blue-emitting emissive layer leads to efficient energy transfer and thus sufficient down-converted red emission at low doping concentrations of the red-emitting dye in the CCLs. It ensures reduced self-quenching of dye molecules and consequently results in efficient red emission. EL measurements show that the peak EQE and the peak power efficiency of the white LECs employing red CCLs reach 5.93% and 15.34 lm W^{-1}, respectively, which are among the highest reported for white LECs. Furthermore, these white LECs exhibit bias-insensitive white EL spectra, which are essential for practical applications, due to nondoped emissive layers. These results confirm that single-layered blue-emitting LECs combined with red-emitting CCLs are one of the potential candidates for efficient and color-stable white light-emitting devices.

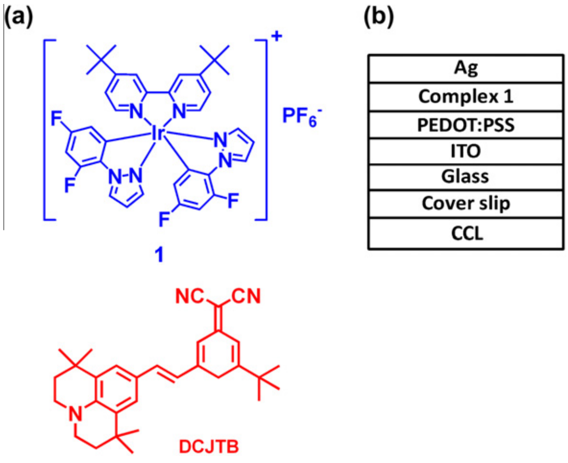

Fig. 1. (a) Molecular structures of the blue-emitting CTMC (1) used in the emissive layer of the LEC and the red-emitting dye (DCJTB) used in the CCL. (b) Schematic structure of the LEC device combined with a CCL.

2. Experiment

2.1. Materials

Molecular structures of the blue-emitting CTMC (complex 1) used in the emissive layer of the LEC and the red-emitting dye DCJTB used in the CCL are shown in Fig. 1(a). The blue-emitting complex 1 $[Ir(dfppz)_2(dtb\text{-}bpy)]^+(PF_6^-)$ (where dfppz is 1-(2,4-difluorophenyl)pyrazole and dtb-bpy is [4,4′-di(*tert-butyl*)-2,2′-bipyridine]) reported previously by Tamayo et al. [24] was used as the emissive material. Complex 1 was synthesized according to the procedures reported in the literature [24]. The red-emitting dye (DCJTB, LumTech) and poly(methyl methacrylate) (PMMA, weight-average molecular weight $M_w = 350{,}000\ \mathrm{g\ mol^{-1}}$, Alfa Aesar) were used as received.

2.2. Photoluminescent characterization

Thin films of the complex 1 for PL studies were spin-coated at 3000 rpm onto quartz substrates using acetonitrile solutions (150 mg/mL). Thin films of PMMA doped with DCJTB (0.3, 0.4 and 0.5 wt.%) were spin-coated at 1000 rpm onto quartz substrates using chlorobenzene solutions (180 mg/mL). The thicknesses of the spin-coated complex 1 and DCJTB-doped PMMA films were c.a. 400 nm and 6 μm, respectively, as measured using profilometry. The absorption spectrum of DCJTB was measured using dichloromethane solutions (10^{-5} M). UV–Vis absorption spectra were recorded using a Hitachi U2800A spectrophotometer. PL spectra were recorded using a Hitachi F9500 fluorescence spectrophotometer. PLQYs for thin-film samples were determined using a calibrated integrating sphere system (Hamamatsu C9920).

2.3. CCL preparation, LEC device fabrication and characterization

The CCLs were spin-coated at 1000 rpm onto cover slips (1.8 cm × 1.8 cm × 0.15 mm) using chlorobenzene solutions (180 mg/mL) of PMMA doped with various concentrations of DCJTB (0.3, 0.4 and 0.5 wt.%). The thickness of the CCL was c.a. 6 μm as measured by profilometry. Indium tin oxide (ITO)-coated glass substrates were cleaned and treated with UV/ozone prior to use. A poly(3,4-ethylenedioxythiophene):poly(styrene sulfonate) (PEDOT:PSS) layer was spin-coated at 4000 rpm onto the ITO substrate in air and baked at 150 °C for 30 min. The emissive layer (~400 nm, as measured by profilometry) was then spin-coated at 3000 rpm from the acetonitrile solutions of complex 1 under ambient conditions. To reduce the turn-on time of the LEC devices, the ionic liquid [$\mathrm{BMIM^+(PF_6^-)}$] (where BMIM is 1-butyl-3-methylimidazolium) of 20 wt.% was added to enhance the ionic conductivity of the emissive layers [22]. The concentration of the solutions used for spin coating of the emissive layers is 150 mg/mL. After spin coating, the samples were then baked at 70 °C for 10 h in a nitrogen glove box (oxygen and moisture levels below 1 ppm), followed by thermal evaporation of a 100-nm Ag top contact in a vacuum chamber (~10^{-6} torr). The schematic diagram of the LEC device combined with a CCL is shown in Fig. 1(b). The LEC device was placed on the top of the cover slip containing a CCL during EL characterization. No adhesive was used between the glass substrate and the cover slip. The electrical and emission characteristics of LEC devices were measured using a source-measurement unit and a Si photodiode calibrated with the Photo Research PR-650 spectroradiometer. All device measurements were performed under a constant bias voltage (3.1, 3.3, 3.5, 5, 7 and 9 V) in a nitrogen glove box. The EL spectra were taken with a calibrated CCD spectrograph.

3. Results and discussions

3.1. Photoluminescent studies

PL spectrum of the films of $\mathrm{[Ir(dfppz)_2(dtb\text{-}bpy)]^+(PF_6^-)}$ (complex 1) containing 20 wt.% $\mathrm{BMIM^+(PF_6^-)}$, which has the same components with those used in the emissive layers of LECs is shown in Fig. 2. These films exhibit blue phosphorescent PL centered at 490 nm. Highly retained PLQY of complex 1 in neat films (0.75) [55] in comparison with that in dilute solutions (1.00) [55] reveals reduced self-quenching in neat films possibly resulting from the sterically bulky di-*tert-butyl* groups of the bipyridine ligand [24], suggesting its suitability for use as the emissive material of neat-film blue-emitting LECs. To achieve efficient energy transfer from the emissive layer of LEC to the CCL layer, the red-emitting material doped in the CCL should exhibit absorption spectrum matched well with the emission spectrum of complex 1. As shown in Fig. 2, good spectral overlap between the absorbance spectra of the red-emitting dye (DCJTB) dispersed in PMMA films (0.3, 0.4 and 0.5 wt.%) and the emission spectrum of the blue-emitting emissive layer (complex 1) would lead to efficient energy transfer and thus sufficient down-converted red emission at low doping concentrations of the red-emitting dye in the CCL layer. Low doping concentrations is beneficial in reducing self-quenching of dopants and consequently results in efficient red emission from the CCL layer. From the data of absorbance, which is defined as $\log_{10}(I_0/I)$ (where I_0 is the intensity of the light before it enters the CCL sample and I is the intensity of the light passed through the CCL sample), the percentages of absorption of the excitation source at 490 nm for CCLs with DCJTB at 0.3, 0.4 and 0.5 wt.% are estimated to be c.a. 50%, 62% and 89%, respectively. The PL spectra of the CCLs doped with various concentrations of DCJTB (0.3, 0.4 and 0.5 wt.%) under an excitation source at 490 nm are also depicted in Fig. 2. All PL spectra were collected under the same excitation intensity. The PL emissions of CCLs doped with 0.3–0.5 wt.% DCJTB center at c.a. 600 nm and exhibit slight bathochromic shift with increased DCJTB concentrations due to enhanced molecular polarization effect [62].

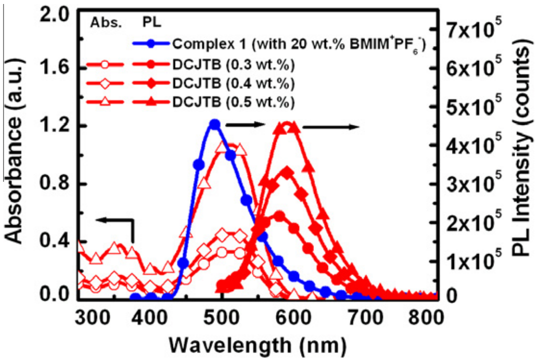

Fig. 2. Absorbance and PL spectra of DCJTB dispersed in PMMA films (0.3, 0.4 and 0.5 wt.%). PL spectrum of films of complex 1 containing 20 wt.% $\mathrm{BMIM^+(PF_6^-)}$ is also shown for comparison.

From Fig. 2, the relative values of integrated PL intensities of CCLs with DCJTB at 0.3, 0.4 and 0.5 wt.% are estimated to be c.a. 46, 64, and 89, respectively. These results reveal that PL intensities of CCLs with 0.3–0.5 wt.% DCJTB are in proportion to the amount of absorption of the excitation source at 490 nm, indicating similar PLQYs of PMMA films doped with DCJTB at 0.3–0.5 wt.%. White emission can be obtained by combining emissions of complex 1 and DCJTB in proper ratios. The PLQY of CCLs doped with 0.3–0.5 wt.% DCJTB were determined to be c.a. 0.6, which is much higher than the PLQYs of previously reported red-emitting CTMCs used in host–guest white LECs (<0.2) [36,42,47,55]. Thus, utilizing CCLs doped with DCJTB to generate red emission would be beneficial in further enhancing device efficiencies of white LECs.

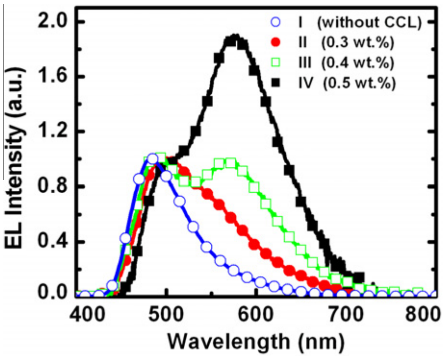

Fig. 3. EL spectra of the white LECs with CCLs doped with various DCJTB concentrations (0.3, 0.4 and 0.5 wt.%) under 3.3 V. EL spectrum of the LECs based on complex 1 without CCLs under 3.3 V is also shown for comparison. Blue emission peaks are normalized for clarity.

3.2. EL characteristics of the white LECs with CCLs

To clarify the EL properties of the white LECs with CCLs, EL characteristics were measured and are summarized in Table 1. The LECs combined with CCLs have the structure of CCL (6 μm)/cover slip (0.15 mm)/glass (0.55 mm)/ITO (120 nm)/PEDOT:PSS (30 nm)/emissive layer [complex 1 (80 wt.%) and BMIM$^+$(PF$_6^-$) (20 wt.%)] (400 nm)/Ag (100 nm), where the CCL/cover slip structure is absent for the reference Device I and the CCLs contain DCJTB of 0.3, 0.4 and 0.5 wt.% for Device II, Device III and Device IV, respectively. The ionic liquid BMIM$^+$(PF$_6^-$) was added in the emissive layer to provide additional mobile ions and to shorten the device response time [22]. The EL spectra of the white LECs with CCLs doped with various DCJTB concentrations (0.3, 0.4 and 0.5 wt.%) under 3.3 V are shown in Fig. 3. EL spectrum of the LECs based on complex 1 without CCLs under 3.3 V is also shown for comparison. For the EL emission coming from complex 1, EL spectra are basically similar to PL spectra, indicating similar emission mechanisms. When CCLs are incorporated with the LEC devices, some blue electrophosphorescence of complex 1 is absorbed and then down-converted to red fluorescence of DCJTB, resulting in a mixture of white emission. As shown in Fig. 3, the relative intensity of the red emission as compared to the blue emission, which was normalized for clarity, is enhanced as the doping concentration of DCJTB in the CCLs increases. It is noted that the red emission enhances more significantly in EL spectra of LEC devices than in PL spectra of CCLs when the doping concentration of DCJTB increases. It is attributed that only excitation light at 490 nm accounts for PL emissions of CCLs while whole EL spectrum of complex 1 can be absorbed by DCJTB molecules to generate red emission. Therefore, by considering the overlap integral of the absorbance spectra of CCLs (peak at c.a. 510 nm) and the PL spectrum of complex 1, which is similar to the EL spectrum of complex 1 [57], relatively more significant enhancing in red emission at higher DCJTB concentrations, e.g., at 0.5 wt.% (Fig. 3), is reasonable in EL spectra. Since absorption of DCJTB results in down-converted red emission, the color of white emission can be feasibly adjusted by tuning the DCJTB concentration in CCLs without altering balance of carrier

Table 1
Summary of the device characteristics of white LECs with red color conversion layers.

Device (DCJTB concentration)[a]	Bias (V)	t_{max} (min)[b]	L_{max} (cd m^{-2})[c]	$\eta_{ext,\ max}$ (%)[d]	$\eta_{p,\ max}$ (lm W^{-1})[e]	Lifetime (min)[f]	CIE (x, y)[g]	CRI[g]
I (without CCL)[h]	3.1	223	7.92	14.47	32.12	130	(0.195,0.362)	–
	3.3	104	23.42	14.35	29.92	46		
	3.5	61	38.33	13.28	26.19	27		
II (0.3 wt.%)	3.1	146	4.63	8.54	23.11	113	(0.295,0.470)	50
	3.3	71	11.90	8.50	21.60	47		
	3.5	51	19.79	7.22	17.23	27		
III (0.4 wt.%)	3.1	129	2.87	5.93	15.34	111	(0.365,0.444)	66
	3.3	103	9.45	5.49	13.35	47		
	3.5	66	16.21	5.53	12.67	23		
IV (0.5 wt.%)	3.1	204	3.34	5.01	14.58	123	(0.435,0.493)	58
	3.3	94	8.47	5.01	13.73	53		
	3.5	47	13.29	4.63	11.90	26		

[a] DCJTB concentrations of the color conversion layers.
[b] Time required to reach the maximal brightness.
[c] Maximal brightness achieved at a constant bias voltage.
[d] Maximal external quantum efficiency achieved at a constant bias voltage.
[e] Maximal power efficiency achieved at a constant bias voltage.
[f] The time for the brightness of the device to decay from the maximum to half of the maximum under a constant bias voltage.
[g] Evaluated from the EL spectra under 3.3 V.
[h] Devices without color conversion layers.

mobilities in the emissive layer, which may deteriorate device efficiencies [55]. Independent color tuning of white EL emission and tailoring of balance of carrier mobilities in the emissive layer would facilitate optimizing device efficiencies of white LECs [55].

Another promising advantage of white LECs with CCLs is bias-insensitive EL spectra. As shown in Fig. 4, the EL spectra of Device III (DCJTB 0.4 wt.%) are approximately the same under biases of 3.1–9.0 V, which correspond to device current densities and maximum brightness of 0.04–16.17 mA/cm^2 and 2.87–184.92 cd/m^2. Commission Internationale de l'Eclairage (CIE) [63] coordinates of these EL spectra are shown in the inset of Fig. 4. No significant color shift in EL spectra was observed for Device III under 3.1–9.0 V since the CIE coordinate migration (Δx, Δy) is less than (±0.009, ±0.005). Slight color shift may be attributed to microcavity effect [64] of thickness variation in solution-processed emissive layer and CCL of each device. Similarly slight color shifts under the same range of bias voltages were also observed for Device II and Device IV. These results reveal good color stability of white LECs with CCLs. In contrast, typical host–guest white LECs usually exhibit significant color shift under similar bias voltages (or current densities). For instance, CIE coordinate migration up to (±0.124, ±0.029) has been reported for white LECs composed of a blue-emitting host CTMC doped with a red-emitting guest CTMC when bias voltage (current density) varied from 2.9 to 3.3 V (0.01–0.12 mA/cm^2) [55]. For host–guest LECs, electrochemically doped regions of the emissive layer result in ohmic contact with metal electrodes and consequently facilitate carrier injection onto both the host and the guest. Hence, both exciton formation on the host followed by host–guest energy transfer and direct exciton formation on the guest induced by charge trapping contribute to the guest emission. The later is more significant under relatively lower biases and thus varying bias condition leads to different fractions of guest emission, which results in color shift in white EL spectrum. This is an inherent characteristic of host–guest white LECs and it is not easy to overcome this obstacle. Separating red-emitting materials from the active layer, e.g., utilizing CCLs, would be one of the promising techniques to achieve color-stable white LECs.

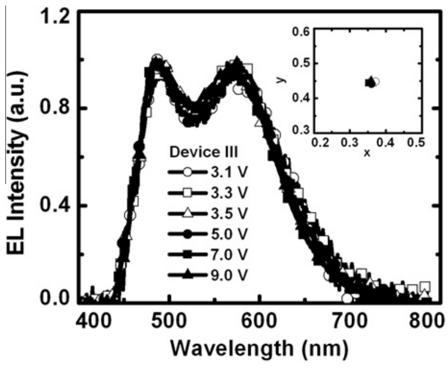

Fig. 4. EL spectra of Device III under various bias voltages. Inset: CIE coordinates of these EL spectra.

To examine the color stability of white LECs with CCLs under various bias voltages, time dependent EL spectra of Device III under 3.1, 3.3 and 3.5 V are shown in Fig. 5(a–c), respectively. For each bias voltage, EL spectra were sampled when the brightness is increasing, approaching the maximum and decreasing finally. The CIE coordinate migrations of the EL spectra of Device III under 3.1, 3.3 and 3.5 V are within (±0.005, ±0.004), (±0.004, ±0.004) and (±0.003, ±0.008), respectively. Slight variation of color change in temporal EL spectra may result from extending of the doped regions and shrinking of the intrinsic layer with time under a bias [18], which perturbs the optical structure due to different refractive index of each layer [64]. However, these color shifts are much smaller than those observed in host–guest white LECs under similar bias ranges [55]. These results confirm white LECs with CCLs

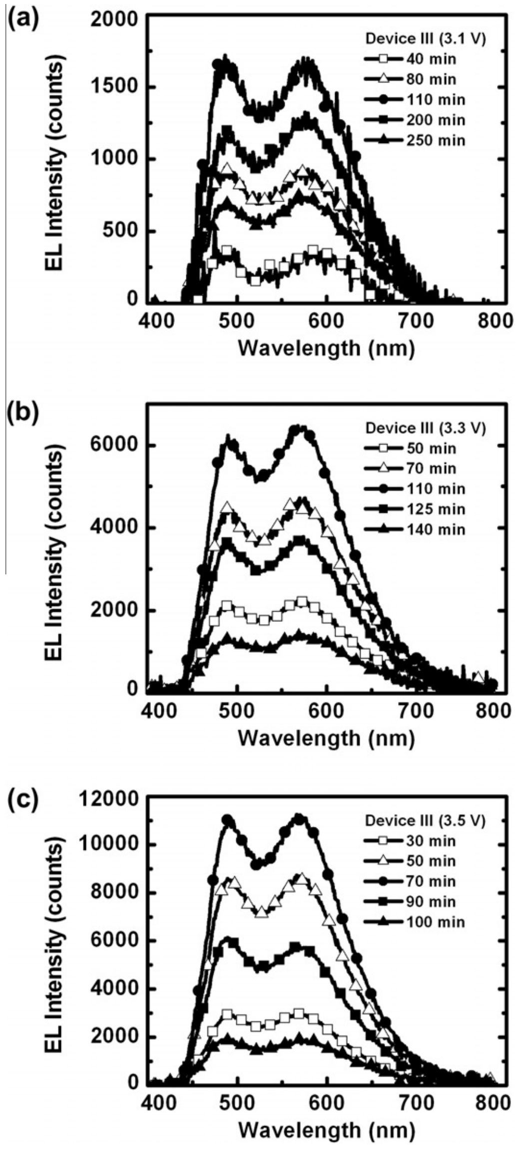

Fig. 5. Time dependent EL spectra of Device III under (a) 3.1 (b) 3.3 and (c) 3.5 V.

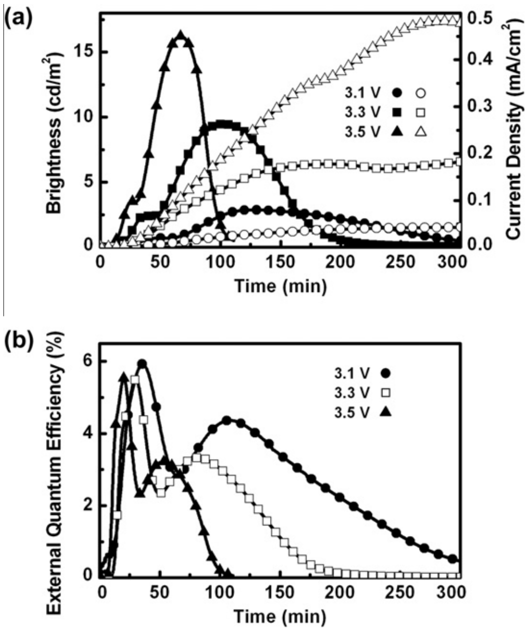

Fig. 6. (a) Brightness (solid symbols) and current density (open symbols) and (b) external quantum efficiency as a function of time under a constant bias voltage of 3.1–3.5 V for Device III.

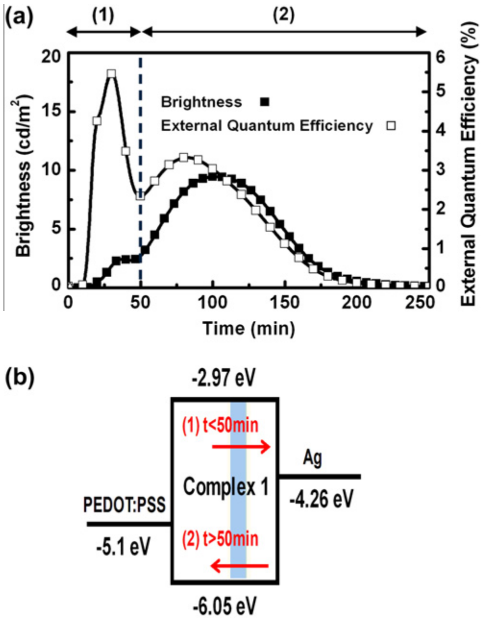

Fig. 7. (a) Brightness (solid symbols) and external quantum efficiency (open symbols) as a function of time under a constant bias voltage of 3.3 V for Device III. Two operation schemes are labeled: (1) $t < 50$ min and (2) $t > 50$ min. (b) Schematic energy levels of complex 1 and work functions of PEDOT:PSS and Ag. Moving of the recombination zone in scheme (1) and (2) are shown in the complex 1 layer.

are capable of providing stable and bias insensitive white EL spectra.

The time-dependent brightness/current density and EQE under constant biases of 3.1–3.5 V for Device III are shown in Fig. 6(a) and (b), respectively. It is noted that unusual phenomena of a shoulder in brightness (e.g., at c.a. 30 min for 3.3 V) and a dip in device efficiency followed by a second rise (e.g., at c.a. 50 min for 3.3 V) were observed in LECs based on complex 1 with a relatively thicker emissive layer (~400 nm). These phenomena were also found in LECs without CCLs (Device I). However, LECs based on complex 1 with relatively thinner emissive layer (~200 nm) did not exhibit such phenomena [55,57]. Thus, this unusual behavior is related to the EL properties of a thicker emissive layer and has nothing to do with the PL properties of CCLs. We propose two schematic operation schemes shown in Fig. 7 to explain such unusual EL properties. Since all LECs under 3.1, 3.3 and 3.5 V showed similar trends in EL properties (Fig. 6), LECs under 3.3 V are discussed for example. As shown in Fig. 7(a), after the bias was applied, the brightness and device efficiency increased with time due to enhanced carrier injection induced by gradually formed *p*- and *n*-type doped layers near electrodes. Initially (scheme (1), Fig. 7(a)), the recombination zone would be relatively nearer the cathode since hole injection (injection barrier is 0.95 eV) is relatively easier than electron injection (injection barrier is 1.29 eV) (Fig. 7(b)). Due to a relatively smaller injection barrier, the required amount of accumulated anions near the anode for ohmic contact of holes would be less than the required amount of accumulated cations near the cathode for ohmic contact of electrons. Ohmic contact of hole would thus take place earlier than ohmic contact of electron. The injection efficiency of holes would consequently increase faster than that of electrons at the initial stage of operation and the recombination zone would be gradually shifted toward the cathode with time (scheme (1), Fig. 7(b)). When the recombination zone is approaching the cathode, exciton quenching near electrode [65] occurs and the device efficiency degrades. As shown in Fig. 7(a), the increasing of brightness with time retarded at 30–50 min and simultaneously the EQE significantly deteriorated. After 50 min, subsequent ohmic contact of electron injection is achieved and thus balanced carrier injection would push back the recombination zone toward the center of the emissive layer (scheme (2), Fig. 7(b)). As shown in Fig. 7(a), after 50 min, the increasing of brightness recovered and the EQE increased again due to reduced exciton quenching near electrode [65]. However, the second peak of EQE is lower than the first one since degradation of complex 1 under electrical operation is continuous. The decrease in brightness and EQE after 100 min may also be rationally attributed to the degradation of the emissive material during the LEC operation [16]. In LECs based on complex 1 with a relatively thinner emissive layer (c.a. 200 nm) [57], the turn-on time was much shorter under similar bias voltages due to much faster accumulation rates of mobile ions under higher electric fields. The difference in time required for ohmic contact of hole and electron would be similar. Furthermore, recombination zone in a thinner emissive layer would be closer to electrodes and exciton quenching would be significant during the whole period of electrical operation. Therefore, LECs based on complex 1 with a relatively thinner emissive layer exhibited lower peak EQEs and did not show unusual electrical properties mentioned above [57].

Thicker emissive layer made by spin coating also leads to large variation in the time required to reach the maximal brightness ($t_{\max}$) between each individual device. As shown in Table 1, $t_{\max}$ (shown as average and variation) of LECs under 3.1, 3.3 and 3.5 V are 176 ± 27%, 87.5 ± 19% and 56.5 ± 18% min, respectively. Larger variation in turn-on time was found in lower bias voltages. Since the emissive layer was deposited by spin coating, spatial variation in thickness of thin film can not be easily avoided. When the applied bias voltage is lower and the film is thicker, the variation in film thickness would have significant effect on the speed of conductive doping processes due to a lower electric field. More time is needed to turn on thicker LECs since the accumulation rate of mobile ions is slower under a lower electric field. However, after the *p*- and *n*-type regions are well established, the EL properties are less dependent on device thickness. Thus maximum current density and consequent device lifetime are similar for LECs under the same bias voltage (Table 1).

Brightness and device efficiency of white LECs with CCLs under the same bias voltage decrease as the DCJTB concentration increases (Table 1). Since the refractive index of PMMA is c.a. 1.50 at 490 nm, which is close to that of the ITO glass substrate and glass cover slips (both of them exhibit refractive indices of ~1.52 at 490 nm), waveguiding of blue light in glass substrate and glass cover slip due to total internal reflection at the interface between glass and PMMA is not significant (critical angle ~81°). Thus, compared with blue-emitting LECs without CCLs, in which glass substrate is next to the air, more blue light can be coupled out of the glass substrate, resulting in excitation of DCJTB and red reemission. However, out-coupling efficiency of red light from the PMMA layer into the air in forward direction is only c.a. 23%, which is estimated by the formula $1/2n^2$ (where $n = 1.49$ for PMMA at 600 nm) [39]. More blue emission from complex 1 transferred to DCJTB leads to more red light trapped in the PMMA layer, which can only be out-coupled into the air from the device sides (lateral directions), consequently deteriorating device efficiencies in the forward direction. The roll-off of device efficiency as the DCJTB concentration increases is significant. Under 3.1 V, the peak EQE (power efficiency) is 8.54% (23.11 lm W^{-1}) when the DCJTB concentration is 0.3 wt.% while the peak EQE (power efficiency) reduces to 5.01% (14.58 lm W^{-1}) as the DCJTB concentration increases to 0.5 wt.% (Table 1). However, the roll-off of brightness as the DCJTB concentration increases is relatively less significant. Under 3.1 V, the brightness is 4.63 cd m^{-2} when the DCJTB concentration is 0.3 wt.% while the brightness retains at 3.34 cd m^{-2} as the DCJTB concentration increases to 0.5 wt.% (Table 1). When the DCJTB concentration increases, the number of total photons from the LEC device in the forward direction reduces while the spectral overlap between the EL spectrum (Fig. 3) and the luminosity function, which centers at 555 nm [66] increases, rendering a higher lumen or candela value. Thus, this effect retards the roll-off in brightness as compared to that in device efficiency. Since some energy loss occurs in CCLs, highly efficient white LECs with CCLs can only be achieved by utilizing highly efficient blue-emitting CTMCs as the emissive materials in LECs. To enhance device efficiencies of white LECs with CCLs, highly efficient complex 1 was used as the emissive material of LECs and the thickness of the emissive layer was increased (c.a. 400 nm) to reduce exciton quenching in the recombination zone near electrodes [65]. The blue-emitting LECs showed high EQEs up to 14.47% under 3.1 V (Table 1). Furthermore, highly efficient red-emitting DCJTB with a high PLQY up to 0.6 was used in the CCLs. Therefore, white LECs with CCLs (0.4 wt.% DCJTB) showing comparable blue and red EL emission (Fig. 3) still exhibited a high EQE (power efficiency) of 5.93% (15.34 lm W^{-1}), which is higher than those of previously reported host–guest white LECs based on a blue-emitting host doped with a red-emitting guest [36,42,47,55]. These results convince that combining blue-emitting LECs with red-emitting CCLs would be a promising technique for providing efficient and color-stable white EL emission in a simple device structure.

Although high device efficiencies can be obtained in white LECs with CCLs, their slow response and short lifetimes prohibit them from practical applications. These drawbacks are common for reported white LECs [36,42,47,55]. Further studies for improving CTMC materials are still required to achieve faster response and better stability for practical applications. In this report, we have utilized the most efficient blue-emitting CTMC ever reported in white LECs [36,42,47,55] as the emissive material and thus high device efficiencies can be obtained. We tend to demonstrate a possible way to mitigate the problem of color instability, which is commonly observed in single-layered host–guest white LECs [36,42,47,55]. Since the research of LEC is still in the early stage and properties of materials used in LECs still have much room for improving, our report is not the total solution for white LECs used in lighting applications. However, with rapid improvements of lifetimes of LECs in recent years [26,27,37,38,44,45,48,49], better LEC materials could be expected and thus white LECs with CCLs will be useful when more stable materials are used in the near future.

4. Conclusions

In summary, we have shown efficient and color-stable white LECs by combining single-layered blue-emitting LECs with red-emitting CCLs on the inverse side of the glass substrate. By judicious choosing of the red-emitting dye doped in CCLs, good spectral overlap between the absorption spectrum of the red-emitting dye and the emission spectrum of the blue-emitting emissive material results in efficient energy transfer and thus sufficient down-converted red emission at low doping concentrations of the red-emitting dye in the CCLs. Self-quenching of dye molecules is reduced when the doping concentrations are low and the red emission is consequently efficient. EL measurements reveal that the peak EQE and the peak power efficiency of the white LECs employing red CCLs reach 5.93% and 15.34 lm W^{-1}, respectively, which are among the highest reported for white LECs. Furthermore, these white LECs exhibit bias-insensitive white EL spectra due to nondoped emissive layers. This device characteristic is essential for practical applications. These results convince that single-layered blue-emitting LECs combined with red-emitting CCLs are one of the potential candidates for efficient and color-stable white light-emitting devices.

Acknowledgement

The authors gratefully acknowledge the financial support from the National Science Council of Taiwan.

References

[1] J. Kido, K. Hongawa, K. Okuyama, K. Nagai, Applied Physics Letters 64 (1994) 815.

[2] B.W. D'Andrade, S.R. Forrest, Advanced Materials 16 (2004) 1585.

[3] X. Gong, S. Wang, D. Moses, G.C. Bazan, A.J. Heeger, Advanced Materials 17 (2005) 2053.

[4] J. Huang, G. Li, E. Wu, Q. Xu, Y. Yang, Advanced Materials 18 (2006) 114.

[5] M.C. Gather, A. Köhnen, K. Meerholz, Advanced Materials 23 (2011) 233.

[6] S. Reineke, F. Lindner, G. Schwartz, N. Seidler, K. Walzer, B. Lüssem, K. Leo, Nature 459 (2009) 234.

[7] Q. Pei, G. Yu, C. Zhang, Y. Yang, A.J. Heeger, Science 269 (1995) 1086.

[8] Q. Pei, Y. Yang, G. Yu, C. Zhang, A.J. Heeger, Journal of the American Chemical Society 118 (1996) 3922.

[9] Y. Yang, Q. Pei, Journal of Applied Physics 81 (1997) 3294.

[10] M. Sun, C. Zhong, F. Li, Y. Cao, Q. Pei, Macromolecules 43 (2010) 1714.

[11] J.K. Lee, D.S. Yoo, E.S. Handy, M.F. Rubner, Applied Physics Letters 69 (1996) 1686.

[12] C.H. Lyons, E.D. Abbas, J.K. Lee, M.F. Rubner, Journal of the American Chemical Society 120 (1998) 12100.

[13] F.G. Gao, A.J. Bard, Journal of the American Chemical Society 122 (2000) 7426.

[14] H. Rudmann, M.F. Rubner, Journal of Applied Physics 90 (2001) 4338.

[15] H. Rudmann, S. Shimada, M.F. Rubner, Journal of the American Chemical Society 124 (2002) 4918.

[16] G. Kalyuzhny, M. Buda, J. McNeill, P. Barbara, A.J. Bard, Journal of the American Chemical Society 125 (2003) 6272.

[17] J.D. Slinker, D. Bernards, P.L. Houston, H.D. Abruña, S. Bernhard, G.G. Malliaras, Chemical Communications (2003) 2392.

[18] H. Rudmann, S. Shimada, M.F. Rubner, Journal of Applied Physics 94 (2003) 115.

[19] J.D. Slinker, A.A. Gorodetsky, M.S. Lowry, J. Wang, S. Parker, R. Rohl, S. Bernhard, G.G. Malliaras, Journal of the American Chemical Society 126 (2004) 2763.

[20] A.R. Hosseini, C.Y. Koh, J.D. Slinker, S. Flores-Torres, H.D. Abruña, G.G. Malliaras, Chemistry of Materials 17 (2005) 6114.

[21] J.D. Slinker, C.Y. Koh, G.G. Malliaras, M.S. Lowry, S. Bernhard, Applied Physics Letters 86 (2005) 173506.

[22] S.T. Parker, J.D. Slinker, M.S. Lowry, M.P. Cox, S. Bernhard, G.G. Malliaras, Chemistry of Materials 17 (2005) 3187.

[23] M.S. Lowry, J.I. Goldsmith, J.D. Slinker, R. Rohl, R.A. Pascal Jr., G.G. Malliaras, S. Bernhard, Chemistry of Materials 17 (2005) 5712.

[24] A.B. Tamayo, S. Garon, T. Sajoto, P.I. Djurovich, I.M. Tsyba, R. Bau, M.E. Thompson, Inorganic Chemistry 44 (2005) 8723.

[25] N. Armaroli, G. Accorsi, M. Holler, O. Moudam, J. Nierengarten, Z. Zhou, R.T. Wegh, R. Welter, Advanced Materials 18 (2006) 1313.

[26] H.J. Bolink, L. Cappelli, E. Coronado, M. Grätzel, M. Nazeeruddin, Journal of the American Chemical Society 128 (2006) 46.

[27] H.J. Bolink, L. Cappelli, E. Coronado, M. Grätzel, E. Ortí, R.D. Costa, P.M. Viruela, M. Nazeeruddin, Journal of the American Chemical Society 128 (2006) 14786.

[28] Q. Zhang, Q. Zhou, Y. Cheng, L. Wang, D. Ma, X. Jing, F. Wang, Advanced Functional Materials 16 (2006) 1203.

[29] M.K. Nazeeruddin, R.T. Wegh, Z. Zhou, C. Klein, Q. Wang, F. De Angelis, S. Fantacci, M. Grätzel, Inorganic Chemistry 45 (2006) 9245.

[30] H.J. Bolink, L. Cappelli, E. Coronado, A. Parham, P. Stössel, Chemistry of Materials 18 (2006) 2778.

[31] H.-C. Su, F.-C. Fang, T.-Y. Hwu, H.-H. Hsieh, H.-F. Chen, G.-H. Lee, S.-M. Peng, K.-T. Wong, C.-C. Wu, Advanced Functional Materials 17 (2007) 1019.

[32] H.-C. Su, C.-C. Wu, F.-C. Fang, K.-T. Wong, Applied Physics Letters 89 (2006) 261118.

[33] J.D. Slinker, J. Rivnay, J.S. Moskowitz, J.B. Parker, S. Bernhard, H.D. Abruña, G.G. Malliaras, Journal of Materials Chemistry 17 (2007) 2976.

[34] L. He, L. Duan, J. Qiao, R. Wang, P. Wei, L.D. Wang, Y. Qiu, Advanced Functional Materials 18 (2008) 2123.

[35] E.Z. Colman, J.D. Slinker, J.B. Parker, G.G. Malliaras, S. Bernhard, Chemistry of Materials 20 (2008) 388.

[36] H.-C. Su, H.-F. Chen, F.-C. Fang, C.-C. Liu, C.-C. Wu, K.-T. Wong, Y.-H. Liu, S.-M. Peng, Journal of the American Chemical Society 130 (2008) 3413.

[37] S. Graber, K. Doyle, M. Neuburger, C.E. Housecroft, E.C. Constable, R.D. Costa, E. Ortí, D. Repetto, H.J. Bolink, Journal of the American Chemical Society 130 (2008) 14944.

[38] H.J. Bolink, E. Coronado, R.D. Costa, E. Ortí, M. Sessolo, S. Graber, K. Doyle, M. Neuburger, C.E. Housecroft, E.C. Constable, Advanced Materials 20 (2008) 3910.

[39] H.J. Bolink, E. Coronado, R.D. Costa, N. Lardiés, E. Ortí, Inorganic Chemistry 47 (2008) 9149.

[40] H.-C. Su, H.-F. Chen, C.-C. Wu, K.-T. Wong, Chemistry - An Asian Journal 3 (2008) 1922.

[41] T.-H. Kwon, Y.H. Oh, I.-S. Shin, J.-I. Hong, Advanced Functional Materials 19 (2009) 711.

[42] L. He, J. Qiao, L. Duan, G.F. Dong, D.Q. Zhang, L.D. Wang, Y. Qiu, Advanced Functional Materials 19 (2009) 2950.

[43] C. Rothe, C.-J. Chiang, V. Jankus, K. Abdullah, X. Zeng, R. Jitchati, A.S. Batsanov, M.R. Bryce, A.P. Monkman, Advanced Functional Materials 19 (2009) 2038.

[44] R.D. Costa, Enrique Ortí, H.J. Bolink, S. Graber, S. Schaffner, M. Neuburger, C.E. Housecroft, E.C. Constable, Advanced Functional Materials 19 (2009) 3456.

[45] R.D. Costa, E. Ortí, H.J. Bolink, S. Graber, C.E. Housecroft, M. Neuburger, S. Schaffnerb, E.C. Constable, Chemical Communications (2009) 2029.

[46] R.D. Costa, F.J. Céspedes-Guirao, E. Ortí, H.J. Bolink, J. Gierschner, F. Fernández-Lázaro, A. Sastre-santos, Chemical Communications (2009) 3886.

[47] L. He, L. Duan, J. Qiao, G. Dong, L. Wang, Y. Qiu, Chemistry of Materials 22 (2010) 3535.

[48] R.D. Costa, E. Ortí, H.J. Bolink, S. Graber, C.E. Housecroft, E.C. Constable, Journal of the American Chemical Society 132 (2010) 5978.

[49] R.D. Costa, E. Ortí, H.J. Bolink, S. Graber, C.E. Housecroft, E.C. Constable, Advanced Functional Materials 20 (2010) 1511.

[50] M. Mydlak, C. Bizzarri, D. Hartmann, W. Sarfert, G. Schmid, L. De Cola, Advanced Functional Materials 20 (2010) 1812.

[51] H.-C. Su, Y.-H. Lin, C.-H. Chang, H.-W. Lin, C.-C. Wu, F.-C. Fang, H.-F. Chen, K.-T. Wong, Journal of Materials Chemistry 20 (2010) 5521.

[52] C.-H. Yang, J. Beltran, V. Lemaur, J. Cornil, D. Hartmann, W. Sarfert, R. Fröhlich, C. Bizzarri, L. De Cola, Inorganic Chemistry 49 (2010) 9891.

[53] H.-F. Chen, K.-T. Wong, Y.-H. Liu, Y. Wang, Y.-M. Cheng, M.-W. Chung, P.-T. Chou, H.-C. Su, Journal of Materials Chemistry 21 (2011) 768.

[54] B. Chen, Y. Li, W. Yang, W. Luo, H. Wu, Organic Electronics 12 (2011) 766.

[55] H.-C. Su, H.-F. Chen, Y.-C. Shen, C.-T. Liao, K.-T. Wong, Journal of Materials Chemistry 21 (2011) 9653.

[56] C.-C. Ho, H.-F. Chen, Y.-C. Ho, C.-T. Liao, H.-C. Su, K.-T. Wong, Physical Chemistry Chemical Physics 13 (2011) 17729.

[57] C.-T. Liao, H.-F. Chen, H.-C. Su, K.-T. Wong, Journal of Materials Chemistry 21 (2011) 17855.

[58] A.R. Duggal, J.J. Shiang, C.M. Heller, D.F. Foust, Applied Physics Letters 80 (2002) 3470.

[59] B.C. Krummacher, V.-E. Choong, M.K. Mathai, S.A. Choulis, F. So, F. Jermann, T. Fiedler, M. Zachau, Applied Physics Letters 88 (2006) 113506.

[60] Y.B. Yuan, S. Li, Z. Wang, H.T. Xu, X. Zhou, Optics Express 17 (2009) 1577.

[61] S.-H. Cho, J.R. Oh, H.K. Park, H.K. Kim, Y.-H. Lee, J.-G. Lee, Y.R. Do, Optics Express 18 (2010) 1099.

[62] V. Bulovic, A. Shoustikov, M.A. Baldo, E. Bose, V.G. Kozlov, M.E. Thompson, S.R. Forrest, Chemical Physics Letters 287 (1998) 455.

[63] Colorimety, Commission Internationale de l'Eclairage (CIE), Paris, 1986.

[64] A. Dodabalapur, L.J. Rothberg, T.M. Miller, E.W. Kwock, Applied Physics Letters 64 (1994) 2486.

[65] K.W. Lee, J.D. Slinker, A.A. Gorodetsky, S. Flores-Torres, H.D. Abruña, P.L. Houston, G.G. Malliaras, Physical Chemistry Chemical Physics 5 (2003) 2706.

[66] G. Wyszecki, W.S. Stiles, Color Science – Concepts and Methods, Quantitative Data and Formulae, second ed., Wiley-Interscience, 2000.